Flutter of Multibay Panels at High Supersonic Speeds

EARL DOWELL*
Massachusetts Institute of Technology, Cambridge, Mass.

The flutter of two-dimensional panels of finite and infinite length on multiple simple supports running in the spanwise direction and equally spaced in the streamwise direction has been investigated theoretically under the assumptions of classical small deflection plate theory and quasi-steady, supersonic aerodynamic theory. An "exact" solution is effected by the method employed by Hedgepeth, Houbolt, and Movchan for the one-bay (two supports) configuration. Specific numerical results are obtained for the one-, two-, three-, four-, five-, and six-bay cases as well as the infinite-bay case with motion of arbitrary spatial periodicity. Comparisons of the present results are made with those of previous investigators. It is found that the previous work is somewhat inaccurate and incomplete. It is concluded that 1) bay number is not a sensitive parameter in the determination of the flutter boundary unless a rather large number of bays is in question, i.e., greater than six; 2) for the multibay configuration, a rather large number of modes (or collocation points) may be required to give accurate results when approximate numerical techniques are employed in the flutter analysis; and 3) the infinite-bay limiting case is not of any great practical importance because of the slow approach to this limiting case. Be that as it may, the restriction in the infinite-bay case to motions that are spatially periodic over an a priori specified number of bays is an artificial one and gives an incomplete description of the physical system.

Nomenclature

A = constant of integration (difference equation), see Eq. (B1)
A_n = constant of integration, see Eq. (A5)
a = speed of sound in air
a_m = speed of sound in panel $= (E/\rho_m)^{1/2}$
B = damping coefficient, also constant of integration, see Eq. (B1)
B_n = constant of integration, see Eq. (A5)
B^* = see Eq. (A7)
C_{j0} = see Eq. (14)
c_{nR} = nondimensional wavespeed in nth bay
C_{jn} = constant of integration for nth bay equation of motion
D = plate stiffness $= Eh^3/12(1 - \nu^2)$
E = modulus of elasticity
E^* = see Eq. (A7)
F^* = see Eq. (A7)
F_N = eigenvalue equation of the N-bay case
G^* = see Eq. (A7)
G = see Eq. (A8)
g_A = aerodynamic damping, $= 0.351\ (1 - \nu^2)^{1/2}\rho/\rho_m a/a_m(L/h)^2 \times M(M^2 - 2)/(M^2 - 1)^{3/2}$
g_S = viscous structural damping, $= 2\zeta_j\omega_j/\omega_0$
g_T = total damping $= g_A + g_S$
H^* = see Eq. (A7)
h = panel thickness
I^* = see Eq. (A7)
L = distance between supports
M = Mach number
m = an integer
N = total number of bays
n = bay number
p = see Eq. (8)
q = dynamic pressure
t = time
U = air velocity
W = panel deflection
W_n = see Eq. (5)
x = distance along chord measured from support to support
Z = mathematical eigenvalue $= (\omega/\omega_0)^2 - i(\omega/\omega_0)g_T$
α = periodicity parameter
γ, δ, ϵ = see Eq. (A2)
ζ_j = critical damping ratio of jth mode
λ = nondimensional dynamic pressure $= 2qL^3/MD$ or $2qL^3/(M^2 - 1)^{1/2}D$
μ = mass ratio $= \rho L/\rho_m h$
ν = Poisson's ratio
ξ = x/L
ρ = air density
ρ_m = panel density
τ = $\omega_0 T$, nondimensional time
ω = frequency
ω_0 = fundamental natural frequency
ω_j = natural frequency of jth mode

Subscripts

n = bay number
m, r, s = dummy subscripts
I = imaginary part
R = real part

Superscript

$\overline{(\ )}$ = conjugate of complex quantity

1. Introduction

ONE of the most disheartening facets of the panel flutter problem in the early investigations of this subject was the poor agreement between theory and experiment (particularly flight flutter tests). In the effort to explain this discrepancy, several modifications to the basic theoretical model (flat, rectangular, isotropic, unstressed panel in a high Mach

Presented as Preprint 64-92 at the AIAA Aerospace Sciences Meeting, New York, January 20–22, 1964; revision received July 13, 1964. This work was supported by the Air Force Office of Scientific Research under Contract No. AF OSR-62-363. The author wishes to express his deep appreciation to John Dugundji for his guidance and help in the preparation of this paper. He would also like to thank Holt Ashley and Marten Landahl for their interest and encouragement. Margot O'Brien undertook the programing of the equations and performed most of the calculations. The present work is a condensed version of a previous report on the subject by the author[1] and is also a portion of a thesis submitted to the Department of Aeronautics and Astronautics in partial fulfillment of the requirements for the degree of Doctor of Science. This work was done in part at the Computation Center of the Massachusetts Institute of Technology.

* Assistant Professor, Department of Aeronautics and Astronautics. Member AIAA.

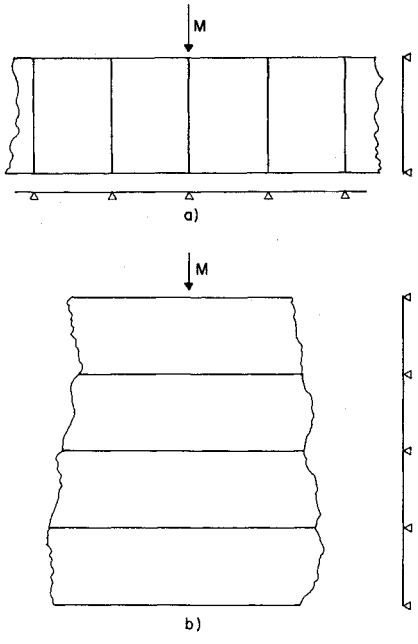

Fig. 1 Multibay configurations.

number flow) were considered. One of these was to consider the effect of adjacent panels. Two configurations in particular have received special attention.

The first configuration is an infinitely wide panel, simply supported on its leading and trailing edges, with equally spaced simple supports in the spanwise direction[2] (see Fig. 1a). It has been shown that this problem may be reduced to a pseudo-aerodynamically two-dimensional panel problem using the "complete," linearized, inviscid aerodynamic operator. For high Mach numbers, this conclusion may be reached by very simple considerations (because of the weak aerodynamic coupling between adjacent spanwise panels).

The second configuration that has been investigated (and the one treated herein) is that of a two-dimensional (i.e., infinitely wide) panel of finite or infinite length with simple supports equally spaced in the streamwise direction[3-6] (see Fig. 1b).

An even more general configuration than either of the forementioned ones (and containing features of both) would be to consider a panel on multiple supports in both the spanwise and streamwise directions. Such a configuration has recently been treated by Zeydel and Kobett[7] for an infinite number of bays in the spanwise direction and one or two bays in the streamwise direction. (A "bay" refers to a panel section between supports.) Their study is directed toward the low supersonic Mach number range.

It is pertinent to point out that, at high Mach numbers, the spanwise coupling between bays is much weaker than that in the streamwise direction. Indeed, this is the justification for the concentration on the effect of streamwise coupling in the present report. It is to be noted, incidentally, that under the assumption of quasi-steady, two-dimensional aerodynamics (high Mach number), the present analysis may be readily extended to include the effects of multiple spanwise supports.

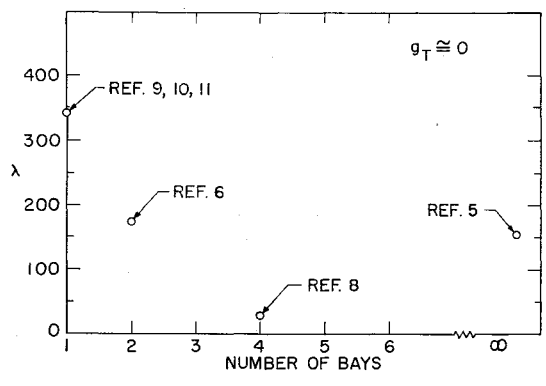

Fig. 2 λ vs N, flutter dynamic pressure vs number of bays.

The two-dimensional, infinitely long, multibay panel has been treated in Refs. 3 and 5 under the assumption of spatial periodicity over two bays (three supports). Within this restriction, the solutions obtained were "exact," i.e., no further mathematical approximations were made. In Ref. 3, the "complete," linearized, inviscid aerodynamic theory was used, whereas in Ref. 5, the "static" approximation was employed. A criticism of the analysis of Ref. 3 was made by Miles,[4] primarily with regard to the appropriateness of the assumption of spatial periodicity over two bays which motivated the work discussed in Ref. 5. In the present work, the restriction to two bay periodicity is removed; the results of the analysis and subsequent numerical work validate in a general way the objections of Miles. Fortunately, as shall be seen, the theoretical model (two-dimensional infinitely long, multibay panel) is of no great practical importance, although it is, perhaps, of some theoretical interest.

The two-dimensional, finite length, multibay panel was investigated by Rodden[6] for the two-bay case (three supports) in his thesis; later, according to Fung,[8] he also studied the four-bay case (five supports). For the two-bay case (and, presumably, for the four-bay case as well), Rodden employed a structural and aerodynamic influence coefficient (finite difference) approach. The "complete" aerodynamic operator was used. The well-known results[8] for the one-bay case as well as Rodden's results for the two- and four-bay cases, and those of Ref. 5 for the infinite-bay case, are shown in Fig. 2 in the form of a nondimensional flutter dynamic pressure for, essentially, zero aerodynamic and zero structural damping. (This figure is merely a replotting of Fig. 9 of Ref. 8.) As may be seen, the two-bay and four-bay results show a significant decrease in flutter dynamic pressure over the one-bay result, with the four-bay result even falling much below the infinite-bay result. In view of the apparent sensitivity of the flutter boundary to bay number and because the analyses and numerical procedures by which the individual results were derived differ somewhat, it was thought desirable to resolve the finite- and infinite-bay cases using the "exact" solution method employed by Hedgepeth,[9] Houbolt,[10] and Movchan[11] for the one-bay case. Quasi-steady aerodynamic theory is used, and thus the results are only valid for high M. A general formulation is made for a two-dimensional finite length panel with an arbitrary number of bays and also the infinite length panel with arbitrary spatial periodicity. Specific numerical results are presented for the one-, two-, three-, four-, five-, and six-bay cases as well as the infinite-bay case.

After the present work began, Ref. 12 became available to the author, wherein the two-bay case is treated by an analogous approach. The present results and those of Mahortikh[12] are identical where comparable.

2. Natural Frequency Spectrum

A brief review of the frequency spectrum of multibay panels will be helpful in understanding the ensuing discussion. The reader is referred to the literature[13, 14] for additional detail.

In Fig. 3, the (nondimensional) frequency for several multibay panels is plotted along a horizontal axis. For $N = 1$, one has the well-known results for a single-bay panel simply supported at either end. The corresponding mode shapes are sine functions. For $N \to \infty$, i.e., an infinite number of bays, the frequency spectrum has a filter-like property with continuous bands of frequencies in the intervals, $m^2 \leq \omega/\omega_0 \leq$

$(m + \frac{1}{2})^2$, where m takes on all integer values. For $\omega/\omega_0 = m^2$, the modes are simple sine functions, whereas for $\omega/\omega_0 = (m + \frac{1}{2})^2$ they are the modes of a single-bay panel clamped at either end.

It is found, for panels with a finite number of bays, that 1) all frequencies lie in the intervals, $m^2 \leq \omega/\omega_0 \leq (m + \frac{1}{2})^2$, 2) the number of frequencies in any one interval is equal to the number of bays, and 3) a frequency that is present for the N-bay case is also present for the NR-bay case, where N and R are (any) integer numbers. Additional numerical values for $N = 1, \ldots, 6$ are shown in Fig. 3.

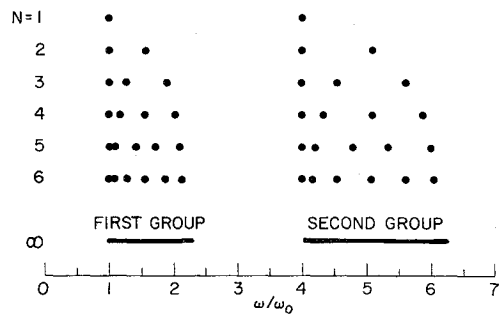

Fig. 3 Natural frequency spectrum.

3. Flutter of a Panel of Finite Length on Equally Spaced Simple Supports

3.1 Formulation

In the following, it will be assumed that the elastic behavior of the plate is adequately described by the classical, small deflection theory and the aerodynamic loading by quasi-steady or the so-called "piston" theory. (The interested reader is referred to Ref. 15 for a discussion of the conditions under which the preceding assumptions are sufficiently accurate.) Thus the equations of motion are

$$(D\partial^4 W_n/\partial x^4) + (\rho_m h \partial^2 W_n/\partial t^2) + (2q/M)[(\partial W_n/\partial x) + (1/U)(\partial W_n/\partial t)] + (B\,\partial W_n/\partial t) = 0 \qquad n = 1, \ldots, N \quad (1)$$

The expression for the aerodynamic pressure is that of "piston" theory. This may be generalized to

$$2q/(M^2 - 1)^{1/2}\{(\partial W_n/\partial x) + [(M^2 - 2)/(M^2 - 1)](1/U)(\partial W_n/\partial t)\}$$

which is the first-order, two-dimensional theory. The use of the latter entails a redefinition of some nondimensional parameters to be introduced subsequently, but changes the analysis in no essential way.

The last term of Eq. (1) includes the effect of "viscous" structural damping. This form has been previously used, for example, by Calligeros and Dugundji.[16] As has been shown in Ref. 16, B may be interpreted as $2\omega_j\zeta_j\rho_m h$ where ω_j and ζ_j are the natural frequency and critical damping ratio, respectively, of the jth mode. It is seen that the assumption of B constant is equivalent to requiring that the critical damping ratio of any mode be inversely proportional to the natural frequency, i.e., $\zeta_j = (\text{const})/\omega_j$. It should be mentioned that the use of other representations of structural damping[17] (e.g., $1 + ig$) may give different results.

For a finite panel, the boundary conditions are as follows: at the first support

$$W_1(0) = \partial^2 W_1(0)/\partial x^2 = 0 \quad (2a)$$

at the last support

$$W_N(L) = \partial^2 W_N(L)/\partial x^2 = 0 \quad (2b)$$

at any intermediate support

$$\left.\begin{aligned} W_n(L) &= 0 \\ W_{n+1}(0) &= 0 \\ \partial W_n(L)/\partial x &= \partial W_{n+1}(0)/\partial x \\ \partial^2 W_n(L)/\partial x^2 &= \partial^2 W_{n+1}(0)/\partial x^2 \\ n &= 1, \ldots, N-1 \end{aligned}\right\} \quad (2c)$$

An exact solution to Eq. (1) subject to the boundary conditions of Eq. (2) is made by the method employed by Hedgepeth,[9] Houbolt,[10] and Movchan,[11] for the one-bay case. The solution is derived in detail in Appendix A.

In the present section, an outline of the solution technique is presented. Equations (1) and (2) are nondimensionalized in the following fashion:

$$\hat{W}_n'''' + \lambda \hat{W}_n' - \pi^4 Z \hat{W}_n = 0 \quad (3)$$

where

$$\lambda \equiv 2qL^3/MD$$
$$Z = (\omega/\omega_0)^2 - i(\omega/\omega_0)g_T \quad (4)$$

and ω_0 is the fundamental panel frequency $= \pi^2(D/\rho_m h L^4)^{1/2}$

$$g_T = g_A + g_s$$
$$g_A = \rho U/M\omega_0\rho_m h = 0.351(1 - \eta^2)^{1/2}(\rho/\rho_m)(a/a_m)(L/h)^2$$
$$g_s = B/\omega_0\rho_m h = 2\zeta_j\omega_j/\omega_0$$

(λ and g_A are here defined using the "piston" theory aerodynamic pressure formula. For their definition using the quasi-steady theory, see the Nomenclature.) The $(\,)'$ denotes differentiation with respect to $\xi = x/L$, and the time-dependence has been assumed to be of the form

$$W_n = \hat{W}_n(\xi)e^{i\omega t} \quad (5)$$

The aerodynamic damping g_A, introduced by Houbolt,[9] may be considered as an alternative to the commonly used mass ratio parameter μ. Their correspondence is given through the relation

$$g_A = 1/\pi^2(\lambda\mu/M)^{1/2} \quad (6)$$

where

$$\mu \equiv \rho L/\rho_m h$$

When the effect of structural damping g_S is to be included, g_A is perhaps a more convenient parameter than μ. Typical values of g_A are given in Ref. 16. For example, for an aluminum panel at sea level, $L/h = 10^2$, $g_A = 0.1$.

Equation (3) has been solved in the classical manner by assuming a solution of the form

$$\hat{W}_n = \sum_{j=1}^{4} C_{jn}e^{p_j\xi} \quad (7)$$

where the p_j are the roots of the polynomial

$$p^4 + \lambda p - \pi^4 Z = 0 \quad (8)$$

Satisfaction of the boundary conditions [Eq. (2)] gives $4N$ homogenous, linear algebraic equations in the unknowns C_{jn}. Setting the determinant of coefficients equal to zero in the usual manner gives the characteristic equation for the eigenvalues. The functional relation may be expressed as

$$F_N(Z;\lambda) = 0 \quad (9)$$

The quantity of physical interest is, of course, ω/ω_0. It may be computed from Eq. (4) as

$$\omega/\omega_0 = ig_T/2 \pm [(g_T/2)^2 + Z]^{1/2} \quad (10)$$

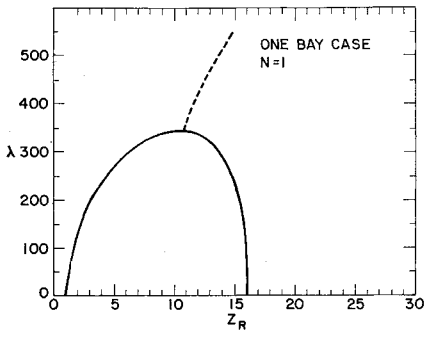

Fig. 4 λ vs Z_R, dynamic pressure vs eigenvalue (real part).

Unstable solutions will occur if the imaginary part of the radical has an absolute value greater than $g_T/2$. The imaginary and real parts of the radical can be evaluated as

$$I_m = \pm\tfrac{1}{2}^{1/2}\{+[(-g_T^2/4 + Z_R)^2 + Z_I^2]^{1/2} + g_T^2/4 - Z_R\}^{1/2}$$

$$Re = Z_I/2I_m \tag{11}$$

Unstable solutions will appear if $g_T/2 < |I_m|$. By routine algebraic manipulation, this inequality reduces simply to

$$g_T < |Z_I|/Z_R^{1/2} \tag{12}$$

At the flutter boundary, $g_T = |Z_I|/Z_R^{1/2}$, it can be shown by direct substitution that $I_m = \pm g_T/2$. Also, it can be shown that, for this value of g_T,

$$|\omega_R/\omega_0| = Z_R^{1/2} \tag{13}$$

Thus, Eq. (13) gives the flutter frequency (nondimensional) in terms of the mathematical eigenvalue, and the inequality, Eq. (12), gives the flutter boundary itself, in the λ, g_T plane. The preceding is essentially the stability parabola concept of Houbolt[10] and Movchan.[11]

Explicit analytical and numerical results have been obtained for $N = 1, \ldots, 6$.

3.2 Some Analytical Results

Before passing on to the numerical results, it is of interest to discuss two of the pertinent analytical properties of the solution. Both of these properties were originally discovered by direct calculation.

1) The complex conjugate of any eigenvalue is also an eigenvalue and its eigenfunction is the complex conjugate of that of the original eigenvalue. This property of the solutions has been proven for the one bay case by Movchan[11] and Krumhaar.[18] The present writer[1] has made the simple extension to the multibay case by an alternate method.

2) Any solution (eigenvalue) of the N-bay case is also a solution of the NR-bay case where N and R are any integers.

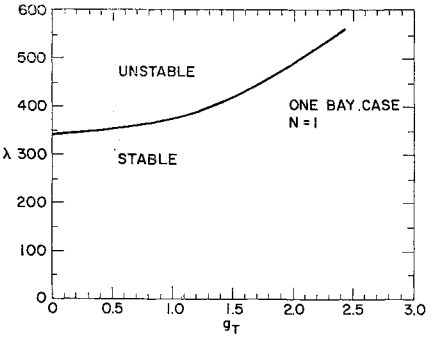

Fig. 5 λ vs g_T, flutter dynamic pressure vs total damping.

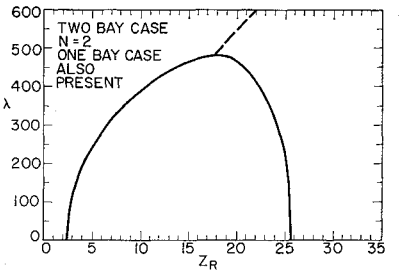

Fig. 6 λ vs Z_R, dynamic pressure vs eigenvalue (real part).

A brief heuristic argument is given here rather than a formal proof. Under the present physical assumptions, ("piston" theory aerodynamics and small deflection plate theory) the effect of one bay on another is felt only through the connecting support. The equation of motion of each bay is independent of any other (i.e., the system of differential equations is coupled only through the boundary conditions). Thus, a solution to the N-bay case will satisfy the equation of motion of any other bay case. However, in general, the boundary conditions will not be compatible. Nevertheless, for the special situation of the NRth-bay case, a solution may be constructed from the (presumably) known solution for the N-bay case as follows.

An N-bay solution is postulated for each of the first, second, ... and Rth groups of N bays. Each of these satisfies the proper differential equation and the boundary conditions at the intermediate supports and the condition of zero deflection and moment at the first and last bay of each group of N bays. They will, however, be determined only within an arbitrary constant and, therefore, there remain R such undetermined constants. R-1 of these are calculated in terms of the Rth by satisfying the remaining condition of continuous slope between the groups of N bays. A formal mathematical proof is given in Ref. 1. This may be considered a generalization of the analogous result for the natural vibrations of multibay panels (see Sec. 2).

3.3 Numerical Results

A. Eigenvalues

The numerical results for each case will be discussed in turn with a summary discussion to follow.

One-bay case: The well-known results for this case are repeated for the sake of completeness and as an easy method of introducing the nomenclature for the subsequent discussion. The numerical results are presented in the form of plots of λ vs Z_R and λ vs $|Z_I|/Z_R^{1/2}$, i.e., g_T. From Figs. 4 and 5 one sees that for λ = 0 the eigenvalues are purely real and remain so until some higher value of λ, called $\lambda_{\text{coalescence}}$, where the first two eigenvalues (ordered according to the magnitude of Z at λ = 0) become equal and then form a

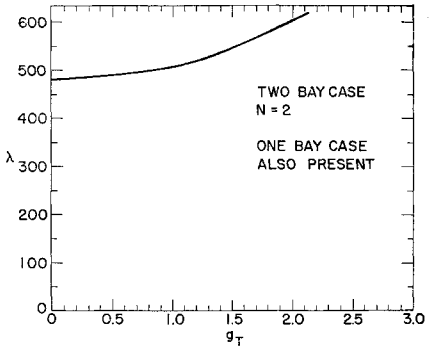

Fig. 7 λ vs g_T, flutter dynamic pressure vs total damping

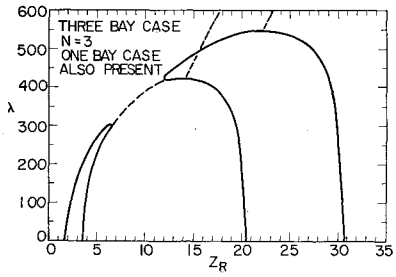

Fig. 8 λ vs Z_R, dynamic pressure vs eigenvalue (real part).

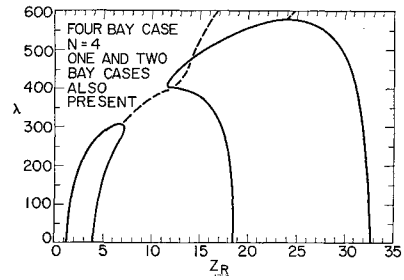

Fig. 10 λ vs Z_T, dynamic pressure vs eigenvalue (real part).

complex conjugate pair. (A dashed line is used for the real part of a complex Z.) For the one-bay case, $\lambda_{coalescence} = 343$. For $g_T = 0$, $\lambda_{flutter} = \lambda_{coalescence}$; however, in general $g_T > 0$, and thus $\lambda_{flutter} > \lambda_{coalescence}$. Values of g_T for practical panels are of the order of unity although there may be a considerable variation for flight in the atmosphere. One sees that, for small values of g_T, the approximation $\lambda_{flutter} \cong \lambda_{coalescence}$ is fairly good. Higher eigenvalues behave in a similar manner although $\lambda_{coalescence}$ for these eigenvalues are much larger (for two-dimensional panels). For example, $\lambda_{coalescence}$ for eigenvalues three and four is approximately 2730.

The stable and unstable regions may be identified by applying the inequality, Eq. (12). For the one-bay case, the regions have been appropriately labeled (see Fig. 6). Such labels have been omitted for $N \geqslant 2$ for the sake of clarity.

Two-bay case: The "one-bay" eigenvalues are solutions to the two-bay case as per the discussion of Sec. 3.2. In Figs. 6 and 7, results are presented only for the remaining two-bay eigenvalues for the sake of clarity. Again, the eigenvalues coalesce in pairs, the first one occurring at $\lambda_{coalescence} = 485$ with the higher modes coalescing at considerably larger λ. As may be seen, the "one-bay" eigenvalues remain the most flutter critical for the two-bay case and thus the flutter boundaries of the one- and two-bay cases, within the present physical approximations, are identical.

Three-bay case: Beginning with the three-bay case, the solutions exhibit some of the behavior unique to the multibay cases. Coalescence now occurs also between roots of a single group; although in some instances these roots subsequently re-emerge as distinct (real) quantities, only later to coalesce with roots of another group.

The "one-bay" eigenvalues are present for this case also. As may be seen from Fig. 8, the two remaining roots of the first group coalesce (and become complex conjugates) at $\lambda = 299$. At $\lambda = 420$, these two roots return to the purely real domain, with one of them shortly thereafter coalescing with the lower root of the second group at $\lambda = 423$. The remaining eigenvalue of the first group finally coalesces with the remaining eigenvalue of the second group at $\lambda = 545$. The return of the eigenvalues to the real domain results in a somewhat different flutter boundary from that observed previously (see Fig. 9). This "looping-back" portion of the boundary has been termed a "weak coalescence"[19] since a small amount of damping g_T will eliminate it. For moderate values of g_T, $g_T \cong 1$, the "one-bay" flutter boundary still remains the most critical (compare Fig. 5).

Four-bay case: The "one-" and "two-bay" solutions are also solutions to the four-bay case. Referring to Figs. 10 and 11, one again sees a coalescence of the two remaining roots of the first group, here at $\lambda = 305$. At $\lambda = 400$, the real part of this complex conjugate pair crosses the (purely real) second root of the second group; however, in this case, no return to the real domain is made. After the crossing is made, a more rapid increase of the imaginary part of the complex conjugate pair with λ is evidenced. Hence, although the coalescence is initially "weak," it later becomes "strong." Also, now the second root of the second group changes direction for $\lambda > 400$ and begins to approach the fourth root of that group, with coalescence taking place at $\lambda = 580$. For small g_T, the flutter boundary of Fig. 11 is the most critical, whereas for moderate g_T, the "one-bay" result is still the most critical.

Five-bay case: The "one-bay" solutions are also solutions for the five-bay case. The remaining roots are shown in Fig. 12 with the flutter boundary given in Fig. 13. The third and fourth roots of the first group coalesce at $\lambda = 295$, the second and fifth at $\lambda = 310$. At $\lambda = 432$, the third and fourth become real again, the third then couples with the third root of the second group at $\lambda = 447$ and the fourth couples with the fourth root of the second group at $\lambda = 520$. The real part of the complex conjugate pair formed by the second and fifth roots of the first group crosses the second root of the second group at $\lambda = 390$, after which there is the characteristic rapid increase of the imaginary part with increasing λ. The second root of the second group reverses its direction shortly thereafter and eventually coalesces with the fifth root of the second group at $\lambda = 600$.

The flutter boundary of Fig. 13 shows that, as for the four-bay case, the critical flutter mode is that given in Fig. 18 for small g_T, whereas for moderate g_T values the critical mode remains that of the "one-bay" case.

Six-bay case: The "one-," "two-," and "three-bay" solutions are also solutions to the six-bay case. The remaining

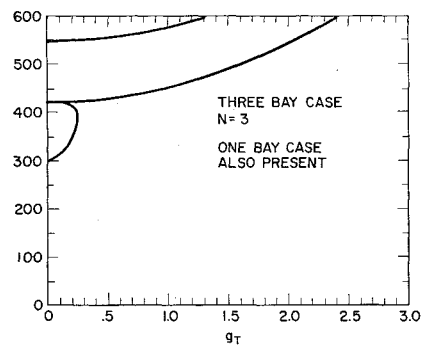

Fig. 9 λ vs g_T, flutter dynamic pressure vs total damping.

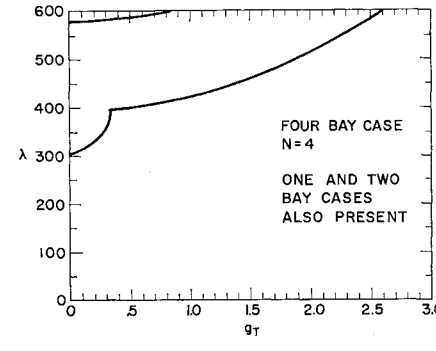

Fig. 11 λ vs g_T, flutter dynamic pressure vs total damping.

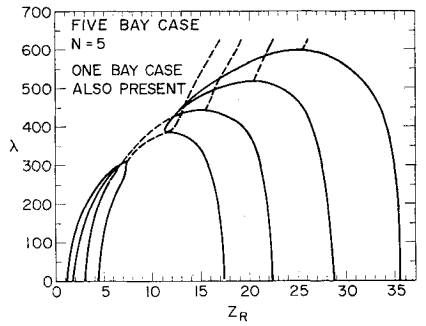

Fig. 12 λ vs Z_R, dynamic pressure vs eigenvalue (real part).

roots are shown in Fig. 14 with the flutter boundary given in Fig. 15. As may be seen, the results are very similar to those discussed for the four-bay case. The two remaining two roots of the first group coalesce at $\lambda = 310$, their real part crosses the second root of the second group at $\lambda = 375$ after which the imaginary part undergoes a more rapid increase with λ and, finally, the second root of the second group changes direction and coalesces with the sixth root of the second group at $\lambda = 605$.

The flutter boundary is qualitatively similar to that of Fig. 11, with the value of g_T for which rapid increases of g_T with λ occurs, being somewhat larger, and the value of λ somewhat smaller. For moderate g_T values, the critical mode remains the "one-bay" case.

B. Eigenfunctions

A few selective calculations have been made for panel mode shapes.[1] For the sake of brevity, they are omitted here. The results for the multibay panel mode shapes show that the amplitude increases from bay to bay with the maximum amplitude occuring near the trailing edge of the last bay.

C. Modal solution

Also, as a matter of interest, a solution employing a modal approach has been made. The panel deflection is expanded in a sine series over the total panel length. The equations of motion are derived via Lagrange's equations and the internal boundary conditions are enforced through the use of Lagrange multipliers. The details of the calculation are given in Ref. 1.

Numerical results have been obtained for the two-bay case using two to eight modes. A comparison between the solutions obtained using various mode combinations shows that the eight-mode solution is well converged as far as the flutter mode is concerned.[1] This should be compared with the four modes required for the one-bay case.[8] For the two-bay case, a four-mode solution is qualitatively incorrect.

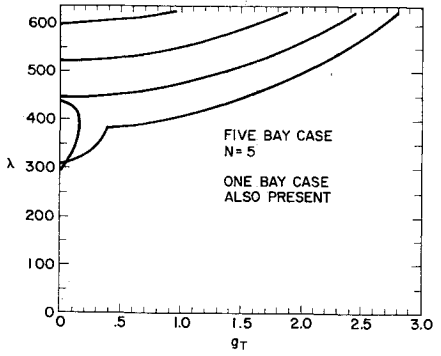

Fig. 13 λ vs g_T, flutter dynamic pressure vs total damping.

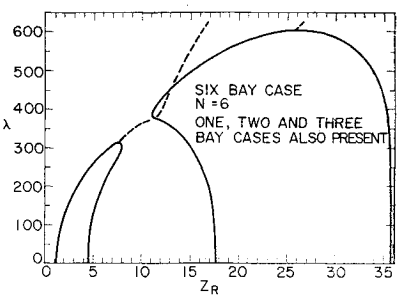

Fig. 14 λ vs Z_R, dynamic pressure vs eigenvalue (real part)

In Figs. 16 and 17, a comparison is made between the eight-mode solution and the "exact" result. As may be seen, the agreement is good excepting the apparent interchanging of roles of the first two modes. That this switching of roles is only apparent is confirmed by calculations of the pertinent mode shapes.[1] The variation in the detailed behavior of the eigenvalues is evidently due to the modal approximation.

It is pertinent to point out that, although the agreement between the model solution and the exact solution is good, strictly speaking, the modal solution has evidently converged to an incorrect answer in the neighborhood of $\lambda_{\text{coalescence}}$. That is, although the difference between $\lambda_{\text{coalescence}}$ as determined by the two methods ("exact" and modal) is only of the order of 5%, still the difference between $\lambda_{\text{coalescence}}$ as determined by two successive modal combinations (seven and eight) is much less.

A twelve-mode solution for the three-bay case was also computed. These results (not shown) are qualitatively incorrect compared to the "exact" solution. Therefore, if one may deduce a trend from the foregoing, it would appear that an increasingly larger number of modes is required to give accurate results as N increases (at least for the modes employed here). This is probably a result of the denser frequency spectrum of the multibay panels.

D. Summary

By way of a summary presentation, λ_{flutter} vs the number of bays has been plotted in Fig. 18 for $g_T = 0$. As may be seen, only a modest reduction in flutter dynamic pressure occurs as a function of bay number. The change would be even less for $g_T > 0$. For any substantial amount of damping, $g_T > 0.4$, the most critical instability is still the "one-bay" result for $N \leq 6$. These results, of course, differ considerably from those presented in Fig. 3. The reason for this discrepancy is apparently the large number of degrees of freedom required for convergence of an approximate modal or finite difference analysis. (More recent calculations by W. P. Rodden[19] have shown the difficulty lies elsewhere. The results of these calculations will be published shortly including a comparison with the present results.)

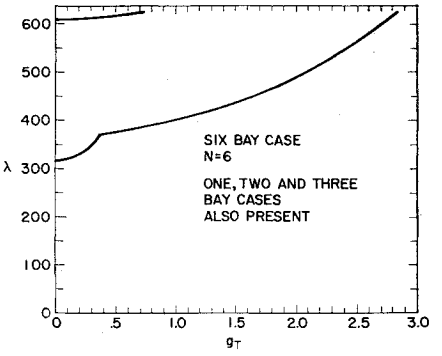

Fig. 15 λ vs g_T, flutter dynamic pressure vs total damping.

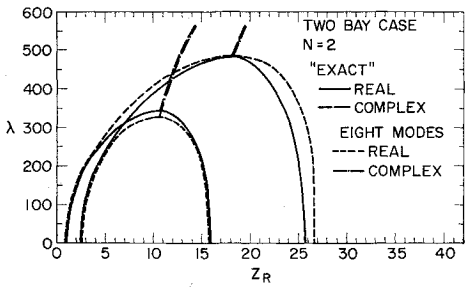

Fig. 16 λ vs Z_R, comparison of "exact" and modal solutions.

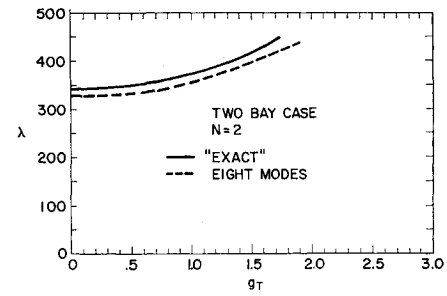

Fig. 17 λ vs g_T, comparison of "exact" and modal solutions.

4. Flutter of a Panel of Infinite Length on Equally Spaced Simple Supports

The results of the multibay finite panel analyses may be interpreted as describing the behavior of a panel pinned at both ends to which additional bays are added at each end. Thus, in the limiting case of a panel on many supports, the total length of the panel becomes infinite.

Another limiting case of possible interest is that in which many bays are added to only one end, i.e., a semi-infinite panel. A brief discussion of this limiting case is contained in Appendix E of Ref. 1. It may be shown that the nontrivial solutions for the eigenvalues of the semi-infinite bay case (though not the eigenfunctions) are identical to those of the infinite-bay case.

4.1 Formulation

The formulation for the infinite-bay panel is, of course, quite similar to that for the finite-bay panel. Indeed, through Eq. (8) they are identical with the exception that the boundary conditions at the first and last support are no longer meaningful. Solutions of the form of Eq. (7) are substituted into the conditions to be satisfied at any intermediate support [Eq. (2c)]. However, instead of the boundary conditions at the "first" and "last" supports, one now has the conditions that the panel deflection remain bounded (finite) as $n \to +\infty$ and $n \to -\infty$. These conditions can be satisfied mathematically by requiring that the constants C_{jn} of Eq. (7) be related to each other through the expressions

$$C_{jn} = e^{i\alpha n} C_{j0} \qquad j = 1, \ldots, 4 \tag{14}$$

where α is an unspecified (real) constant, and C_{j0} is associated with the 0th or reference bay. Specification of a panel deflection shape of this form is essentially a requirement that the panel motion be spatially periodic.

It is of some interest to digress briefly to consider the physical meaning of α in Eq. (14). It is, of course, related to the number of bays over which periodicity exists. Before describing this relationship, however, two properties of the eigenvalues Z for fixed values of λ should be noted, namely,

$$Z(\lambda, \alpha) = Z(\lambda, \alpha - 2\pi) \tag{15}$$

$$Z(\lambda, \alpha) = \bar{Z}(\lambda, -\alpha) \tag{16}$$

The first of these equations is readily deduced from the periodic character of α in Eq. (14); the second, involving the complex conjugate Z, can be deduced from the governing differential equations and boundary conditions.[1] Thus, because of these two properties, only the limited range, $0 \leq \alpha \leq \pi$, need be investigated.

There are two pertinent questions to be asked. The first is, for a given α, what is the number of bays, n^*, over which periodicity exists? This relation is given by

$$n^* = 2\pi R/\alpha \tag{17}$$

where R is any positive integer that permits n^* to take on integer values. For example, for $\alpha = \frac{5}{6}\pi$, $n^* = 12, 24, 36, \ldots$. The minimum value of n^*, in this case $n^* = 12$, will usually be of greatest interest.

The second question one may ask is the converse of the first, namely, what values of α give solutions which are periodic over a specified number of bays, n^*? This relation is given by

$$\alpha = 2\pi R/n^* \tag{18}$$

where R now may take on all integer values from 1 to n^*. (Values of R greater than n^* give values of α greater than 2π and thus, from Eq. (15), merely repeat solutions already obtained.) For example, for $n^* = 6$, the appropriate α's would be

$$\alpha = \pi/3, 2/3\pi, \pi, 4/3\pi, 5/3\pi, 2\pi$$

or equivalently, making use of Eq. (15),

$$\alpha = \pi/3, 2/3\pi, \pi, -2/3\pi, -\pi/3, 0$$

In Refs. 3 and 5, the restriction was made that the motion be periodic over two bays, i.e., $\alpha = \pi$ and $\alpha = 0$. (The details of the formulations of Ref. 3 and 5 differ somewhat from the present one.)

Returning now to the problem formulation, one substitutes Eq. (14) into Eqs. (7) and (2c) which leads to four linear, homogeneous, algebraic equations in the C_{j0}. Setting the determinant of coefficients equal to zero results in a characteristic equation for the eigenvalues which takes the form

$$F_\infty(Z;\ \lambda, \alpha) = 0 \tag{19}$$

An explicit form for this equation, convenient for computation, is derived in Appendix B.

4.2 An Analytical Result

Recalling the two analytical properties discussed in Sec. 3.2 for the finite multibay panel, the second, regarding the presence of the N-bay solutions in the NRth-bay case, is irrelevant for the infinite-bay panel. However, the first, regarding the occurance of eigenvalues as complex conjugates,

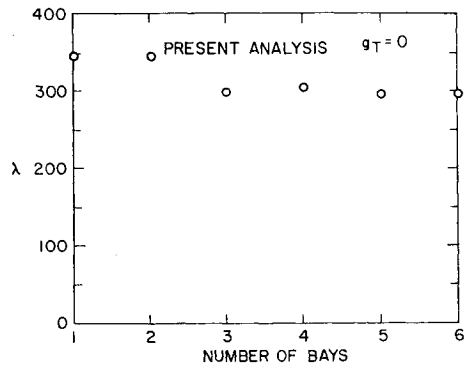

Fig. 18 λ vs N, flutter dynamic pressure vs number of bays.

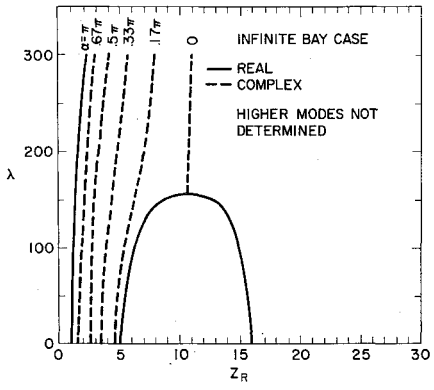

Fig. 19 λ vs Z_R, dynamic pressure vs eigenvalue (real part).

is of some interest, and a derivation or demonstration of this property is presented in Ref. 1.

As will be seen subsequently, the "one-," "two-," "three-," "four-," etc., bay results are not present in the infinite-bay result. The question arises, why not? Instead of giving a completely rigorous answer, the following plausible explanation is offered.

We have restricted ourselves to panel motions that are bounded at infinity and thus are periodic over some number of bays. All such solutions are contained in the present infinite-bay formulation and thus the absence of the "one-," "two-," "three-," "four-," etc., bay results implies they are not bounded at infinity or periodic. This may be verified directly for the "one-" and "two-" bay results from an examination of the mode shapes at $\lambda = \lambda_{\text{coalescence}}$.[1] As the bay number increases, the panel amplitude increases from bay to bay without limit. Presumably this is true of the other finite bay solutions as well.

The question remains, in what manner do the finite-bay results approach those of the infinite bay? It is conjectured that the "new solutions" of the finite-bay cases (the "new" solutions" being here defined as those which do not occur for a smaller number of bays) show less and less amplitude increase from bay to bay as the total number of bays increases. Thus, in the limit, there would be no amplitude variation at all, and the motion would be spatially periodic.

The preceding discussion is intended to be suggestive rather than conclusive. The manner in which the finite-bay case approaches the infinite-bay case remains an open question.

4.3 Numerical Results

Several values of α in the interval $0 \leq \alpha \leq \pi$ have been selected and the corresponding eigenvalues determined for various λ. (The solutions for $\pi < \alpha \leq 2\pi$ may be obtained from these per the discussion of the previous section.) The results are presented graphically in Figs. 19 and 20.

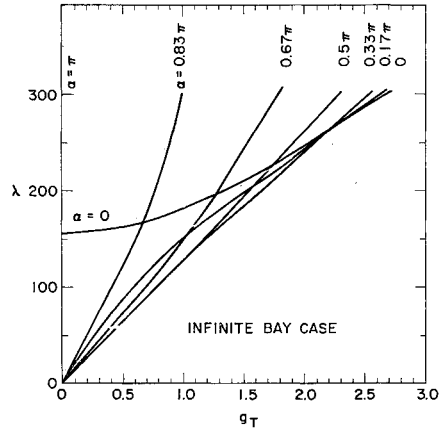

Fig. 20 λ vs g_T, flutter dynamic pressure vs total damping.

For $\alpha = 0, \pi$, and no damping, $g_T = 0$, the present results are in agreement with those of Ref. 5. In the cited reference, an argument was made to the effect that for $g_T = 0$, the only possible solutions to the problem are periodic over two bays for $\lambda \neq 0$. This actually is the case only under the further restriction that one seeks purely real eigenvalues. The consideration of complex eigenvalues demonstrates that infinitely many other solutions exist, and in fact, for $g_T \to 0$, the flutter dynamic pressure $\lambda_{\text{flutter}} \to 0$. For finite values of damping, the flutter dynamic pressure $\lambda_{\text{flutter}} > 0$.

For the $\alpha = \pi$ solution, the panel is stable for λ's up to at least 300. For the $\alpha = 0$ solution, there is a coalescence of the usual type at $\lambda = 154$ of the "last" root of the first group with the "first" root of the second group.† For the $0 < \alpha < \pi$ solutions, "coalescence" occurs at $\lambda = 0$, thus giving unstable motion for $\lambda > 0$ when $g_T = 0$ (see Figs. 19 and 20).

It should, perhaps, be emphasized that each of the curves of Fig. 20 divide the λ, g_T plane into stable and unstable regions for a particular mode (particular α). The "practical" flutter boundary is given by the envelope of these curves which gives the smallest λ for a specified g_T. The flutter mode, characterized by the α that gives the smallest λ, is dependent on damping g_T (see Fig. 20). For $g_T > 2.5$, the flutter mode becomes that associated with $\alpha = 0$; however, for smaller values of g_T, the flutter mode is associated with $0 < \alpha < 0.5\pi$.

Amplification ratios for $\lambda > \lambda_{\text{flutter}}$ have been computed for the one-bay and infinite-bay cases in order to compare the relative severity of the instabilities. The results[1] show that they are of the same order of magnitude.

5. Conclusions and Recommendations

The major conclusions to be drawn from the present study of multi bay panels are:

1) Bay number is not a sensitive parameter in the determination of the flutter boundary unless a rather large number of bays is in question, i.e., $N > 6$.

2) For the multibay configuration, a large number of modes (or collocation points) may be required to give accurate results when approximate numerical techniques are employed in the flutter analysis. This type of behavior would appear to occur for a significant number of panel structures and reemphasizes the importance of performing a convergence study when modal or finite difference techniques are employed.

3) The infinite-bay case (or semi-infinite-bay case), although a valid physical and mathematical limiting case for the panel consisting of very many bays, is not of any great practical importance because of the slow approach to this limiting case. Be that as it may, the restriction in the infinite-bay case to motions that are spatially periodic over an a priori specified number of bays is an artificial one and gives an incomplete description of the physical system.

Extensions to the present analysis and calculations could be made to include the effects of 1) finite width (a multibay spanwise configuration may be reduced to a single-bay spanwise configuration); 2) uniform in-plane stresses; 3) nonuniformities from bay to bay, such as lengths, stiffnesses, etc.; and 4) different panel support conditions. The last of these would appear to be the most important and most interesting. In particular, it would be possible, using the present technique, to analyze more rigorously the dynamic behavior of panels with supports of finite stiffness in translation and rotation.

† Both the $\alpha = \pi$ and $\alpha = 0$ results were obtained in Ref. 5; however, here all values of α (and thus bay periodicities ≥ 2) are considered as well as $g_T \neq 0$.

Appendix A: Finite Panel Eigenvalue Equations

First we consider the polynominal

$$p^4 + \lambda p - \pi^4 Z = 0 \tag{A1}$$

Following Hedgepeth[8] and Houbolt,[9] we write the roots of Eq. (A1) in the form

$$\begin{aligned} p_1 &= -\gamma + \epsilon \qquad p_2 = -\gamma - \epsilon \\ p_3 &= \gamma + i\delta \qquad p_4 = \gamma - i\delta \end{aligned} \tag{A2}$$

From Eqs. (A2) and (A1), the following relations may be determined

$$\begin{aligned} \delta &= (\lambda/4\gamma + \gamma^2)^{1/2} \\ \epsilon &= (\lambda/4\gamma - \gamma^2)^{1/2} \\ Z &= 1/\pi^4(\gamma^2 + \delta^2)(-\gamma^2 + \epsilon^2) \end{aligned} \tag{A3}$$

This form proves convenient for computation, as γ, λ may be chosen and δ, ϵ, and Z computed directly, thus avoiding an explicit factoring of Eq. (A1). Alternatively, one may manipulate Eq. (A3) to give a cubic in γ^2 with Z and λ as parameters, viz.,

$$64\gamma^6 + 16\gamma^2\pi^4 Z - \lambda^2 = 0 \tag{A4}$$

This cubic is readily handled by machine computation. A proper choice of root must be made of course ($\gamma \to 0$ as $\lambda \to 0$).

A deflection shape of the form

$$\begin{aligned} \hat{W}_n = {} & A_n[e^{\gamma(1-\xi)} \sin\delta \sinh\epsilon\xi - e^{-\gamma(1-\xi)} \sinh\epsilon \sin\delta\xi] + \\ & B_n[e^{-\gamma\xi} \sin\delta \sinh\epsilon(1-\xi) - e^{\gamma\xi} \sinh\epsilon \sin\delta(1-\xi)] \end{aligned} \tag{A5}$$

is assumed. This form satisfies the differential equations [Eq. (3)] and the boundary conditions specifying zero deflection at each support. This has been used previously by Hedgepeth[9] and may be deduced from the more general form of Eq. (7). The satisfaction of the remaining boundary conditions gives the following set of equations:

$$\left.\begin{aligned} B^*A_1 - E^*B_1 &= 0 \qquad \text{[from Eq. (2a)]} \\ I^*A_n + H^*B_n - G^*A_{n+1} - J^*B_{n+1} &= 0 \\ F^*A_n + D^*B_n + B^*A_{n+1} - E^*B_{n+1} &= 0 \\ n = 1, \ldots, N-1 \qquad &\text{[from Eq. (2c)]} \\ F^*A_N + D^*B_N &= 0 \qquad \text{[from Eq. (2b)]} \end{aligned}\right\} \tag{A6}$$

where

$$\left.\begin{aligned} B^* &= 2\gamma[\epsilon e^{\gamma} \sin\delta + \delta e^{-\gamma} \sinh\epsilon] \\ E^* &= 2\gamma[\epsilon \sin\delta \cosh\epsilon + \delta \sinh\epsilon \cos\delta] + [\epsilon^2 + \delta^2] \sin\delta \sinh\epsilon \\ I^* &= -2\gamma \sinh\epsilon \sin\delta + \epsilon \sin\delta \cosh\epsilon - \delta \sinh\epsilon \sin\delta \\ H^* &= -\epsilon e^{-\gamma} \sin\delta + \delta e^{\gamma} \sinh\epsilon \\ G^* &= \epsilon e^{\gamma} \sin\delta - \delta e^{-\gamma} \sinh\epsilon \\ J^* &= -2\gamma \sin\delta \sinh\epsilon - \epsilon \sin\delta \cosh\epsilon + \delta \sinh\epsilon \cos\delta \\ F^* &= -2\gamma[\epsilon \sin\delta \cosh\epsilon + \delta \sinh\epsilon \cos\delta] + [\epsilon^2 + \delta^2] \sin\delta \sinh\epsilon \\ D^* &= 2\gamma[\epsilon e^{-\gamma} \sin\delta + \delta e^{\gamma} \sinh\epsilon] \end{aligned}\right\} \tag{A7}$$

Following Miles,[12] one might consider Eq. (A6) as two first-order difference equations for the A_n and B_n with associated boundary conditions; however, for the present purposes, it proves expedient to treat the A_n and B_n as constants of integration and form the characteristic equation by setting their determinant of coefficients equal to zero. For the interested reader, a discussion of the difference-differential equation approach is included in Appendix E of Ref. 1. Here, however, a direct expansion of the characteristic determinant will be used. Such an expansion of the determinant shows that a convenient recurrence formula may be written which relates the characteristic equation of the N-bay case to that of a smaller number of bays. Defining F_N as the characteristic determinant of the N-bay case, we have

$$\begin{aligned} F_N &= \psi F_{N-1} + F_1 G_N \\ G_N &= \Phi F_{N-2} + K G_{N-1} \end{aligned} \tag{A8}$$

with the "initial" conditions

$$F_0 = 0 \qquad F_1 = B^*D^* + E^*F^*$$

where

$$\begin{aligned} \psi &= B^*H^* + E^*I^* \\ \Phi &= G^*H^* - I^*J^* \\ K &= G^*D^* - F^*J^* \end{aligned}$$

Further elimination of G_N from Eq. (A8) leads to the recurrence relation

$$F_N = (\psi + K)F_{N-1} + (\Phi F_1 - \psi K)F_{N-2} \tag{A9}$$

More explicit results are listed below for $N = 1, \ldots, 6$:

$$\begin{aligned} F_1 &= B^*D^* + E^*F^* \\ F_2 &= F_1[\psi + K] \\ F_3 &= F_1[\psi(\psi + K) + \Phi F_1 + K^2] \\ F_4 &= F_1[\psi + K][\psi^2 + 2\Phi F_1 + K^2] \\ F_5 &= F_1\{(\psi + K)[\psi(\psi^2 + 2\Phi F_1 + K^2) + \Phi F_1\psi] + [\Phi^2 F_1^2 + \Phi F_1 K^2 + 2K^2 F_1\Phi + K\Phi F^4\psi + K_1]\} \\ F_6 &= F_1[\psi + K][\psi(\psi + K) + \Phi F_1 + K^2] \times [\psi^2 - \psi K + 3\Phi F_1 + K^2]\ddagger \end{aligned}$$

In examining the F_N, it will be noted that the one-bay result is a factor in all of the other results, the two-bay result is a factor for $N = 4$ and 6, and the three-bay result is a factor in the six-bay case; this, of course, is in agreement with the more general result discussed in Sec. 3.2.

Finally, the computation procedure to determine the eigenvalues Z of F_N is as follows:

For fixed λ, Z is chosen and γ, ϵ, and δ are computed. (Alternatively γ is chosen and Z, ϵ, and δ are computed.) Intermediary calculations are performed to determine B^*, etc., and ψ, etc. Finally, F_N is computed. In general, F_N will not be zero, and another value of Z (or γ) must be chosen and F_N recomputed until a zero of F_N is determined with acceptable accuracy. In the present calculations, this was three or four significant figures for the complex roots and two or three for the real roots.

It is to be noted that Z, and thus F_N, will in general be complex numbers; an iteration scheme based on the method used in Ref. 20 was employed to determine the (complex) zeros of F_N. The eigenfunctions have been computed in the usual manner.

Appendix B: Infinite Panel Eigenvalue Equation

For the infinitely long panel, the first and last of Eq. (A6) are disregarded, and in the remaining two equations of Eq. (A6) we set

$$\begin{aligned} A_n &= Ae^{i\alpha n} \\ B_n &= Be^{i\alpha n} \end{aligned} \tag{B1}$$

‡ The author is grateful to Margot O'Brien who determined this factored form.

in order to satisfy the boundary conditions at infinity, where α is a real number. Substitution of Eq. (B1) into these two remaining equations gives

$$[I^* - e^{i\alpha}G^*]A + [H^* - e^{i\alpha}J^*]B = 0$$
$$[F^* + e^{i\alpha}B^*]A + [D^* - e^{i\alpha}E^*]B = 0 \quad \text{(B2)}$$

Again the characteristic equation is obtained by setting the determinant of coefficients equal to zero. This equation may be written as a quadratic in $e^{i\alpha}$, viz.,

$$F_\infty = e^{i2\alpha}[E^*G^* + B^*J^*] + e^{i\alpha}[-I^*E^* - G^*D^* - H^*B^* + J^*F^*] + [I^*D^* - F^*H^*] = 0 \quad \text{(B3)}$$

This was the computational form used in the present work. Again, eigenfunctions may be computed for a specified α and λ using standard methods.

References

[1] Dowell, E., "The flutter of multi-bay panels at high supersonic speeds," Massachusetts Institute of Technology, Aeroelastic and Structures Research Lab. TR 112-1, Air Force Office of Scientific Research AFOSR 5327 (August 1963).

[2] Luke, Y. L. and St. John, A., "Supersonic panel flutter," Wright Air Development Center TR 57-252 (July 1957).

[3] Hedgepeth, J. M., Budiansky, B., and Leonard, R. W., "Analysis of flutter in compressible flow of a panel on many supports," J. Aeronaut. Sci. **21**, 475–486 (1954).

[4] Miles, J. W., "On the aerodynamic stability of thin panels," J. Aeronaut. Sci. **23**, 771–780 (1956).

[5] Leonard, R. W. and Hedgepeth, J. M., "On the flutter of infinitely long panels on many supports," J. Aeronaut. Sci. **24**, 381–383 (1957).

[6] Rodden, W. P., "The flutter of two-dimensional, flat panels with equally spaced supports in a supersonic flow," Univ. of California, Los Angeles, Ph.D. Thesis (October 1, 1957).

[7] Zeydel, E. F. E. and Kobett, D. R., "The flutter of flat plates with partially clamped edges in the low supersonic region," IAS Paper 63-25 (January 1963).

[8] Fung, Y. C. B., "A summary of the theories and experiments on panel flutter," Air Force Office of Scientific Research TN 60-224 (May 1960).

[9] Hedgepeth, J. M., "On the flutter of panels at high Mach numbers," J. Aeronaut. Sci. **23**, 609–610 (1956).

[10] Houbolt, J. C., "A study of several aerothermoelastic problems of aircraft structures," Doctoral Thesis, Eidgenössische Technische Hochschule, Zurich (1958).

[11] Movchan, A. A., "On vibrations of a plate moving in a gas," Prikl. Mat. Mekh. **20**, 211–222 (1956).

[12] Mahortikh, Z. K., "Stability of multi-bay panels in a high supersonic flow," Izv. Akad. Nauk SSSR, Otd. Tech. Nauk, Mech. i Mashinostr., 174–177 (March-April 1959).

[13] Miles, J. W., "Vibrations of beams on many supports," *Proceedings of the American Society of Civil Engineers* (American Society of Civil Engineers, Ann Arbor, Mich., 1956), Vol. 82, no. EM-1, Paper 863.

[14] Ayre, R. S. and Jacobsen, L. S., "Natural frequencies of continuous beams of uniform span length," J. Appl. Mech. **72**, 391–395 (1950).

[15] Dowell, E. H. and Voss, H. M., "Experimental and theoretical panel flutter studies in the Mach number range 1.0 to 5.0" (report confidential, title unclassified), Aeronautical Systems Div. ASD-TDR-63-449 (June 1963); also AIAA Preprint 64-491 (1964).

[16] Calligeros, J. and Dugundji, J., "Supersonic flutter of rectangular orthotropic panels with arbitrary orientation of orthotropicity," Massachusetts Institute of Technology, Aeroelastic and Structures Research Lab. TR 74-5, Air Force Office of Scientific Research AFOSR 5328 (June 1963).

[17] Johns, D. J. and Parks, P. C., "Effect of structural damping on panel flutter," Aircraft Eng. **32**, 304–308 (October 1960).

[18] Krumhaar, H., "Supersonic flutter of a cylindrical shell of finite length," Air Force Office of Scientific Research TN 59-45, California Institute of Technology (October 1961).

[19] Rodden, W. P., private communication (January 1964).

[20] Runyan, H. L. and Watkins, C. E., "Flutter of a uniform wing with an arbitrary placed mass according to a differential equation analysis and a comparison with experiment," NACA TR 966 (1950).